

# Comparison of fish skins as alternative biological skin models for skin permeability study

Kritsanaporn Tansathien<sup>1</sup>, Praneet Opanasopit<sup>2</sup>, Prasopchai Patrojanasophon<sup>2</sup>, and Mont Kumpugdee-Vollrath<sup>3\*</sup>

<sup>1</sup> Department of Pharmaceutical Technology, Faculty of Pharmaceutical sciences, Huachiew Chalermprakiet University, Samut Prakarn 10540, Thailand

<sup>2</sup> Department of Industrial Pharmacy, Faculty of Pharmacy, Silpakorn University, Nakhon Pathom 73000, Thailand

<sup>3</sup> Department of Pharmaceutical and Chemical Engineering, Berliner Hochschule für Technik, Berlin 13353, Germany

## ABSTRACT

**\*Corresponding author:**  
Mont Kumpugdee-Vollrath  
[vollrath@bht-berlin.de](mailto:vollrath@bht-berlin.de)

**Received:** 18 July 2023  
**Revised:** 15 October 2023  
**Accepted:** 17 October 2023  
**Published:** 29 December 2023

**Citation:**  
Tansathien, K., Opanasopit, P., Patrojanasophon, P., and Kumpugdee-Vollrath, M. (2023). Comparison of fish skins as alternative biological skin models for skin permeability study. *Science, Engineering and Health Studies*, 17, 23050016.

Animal skins are generally used instead of human skin to evaluate drug percutaneous permeation due to ethical and practical reasons. This study aimed to investigate the feasibility of using fish skins, including trout (*Salmo trutta*), Norwegian salmon (*Salmo salar*), BIO salmon (*Salmo salar*), and bighead catfish (*Clarias macrocephalus*) as alternatives. Caffeine was selected as a model drug. The Franz-diffusion apparatus was used for *in vitro* skin permeation test, evaluating parameters such as cumulative permeation profile, permeation flux, permeation coefficient, and lag-time. Skin composition was determined using Fourier-transform infrared spectroscopy. The results revealed that bighead catfish skin exhibited the highest cumulative caffeine permeation, while Norwegian salmon skin closely matched the skin permeability parameters of Strat-M<sup>®</sup>. Based on the permeability parameters and barrier compositions, Norwegian salmon skin demonstrated characteristics similar to Strat-M<sup>®</sup>.

**Keywords:** fish skin; trout; salmon; catfish; skin permeation

## 1. INTRODUCTION

Transdermal delivery stands as an important alternative for drug administration, providing improved drug bioavailability, increased patient compliance, avoidance of first-pass metabolism, heightened safety, and the potential for self-administration (Ramadon et al., 2022). Although human skin is the best membrane for *in vitro* permeability investigation, its use is constrained by ethical, practical, and economical considerations. Consequently, finding alternatives to human skin has become a challenge. Researchers have explored various substitutes such as pig,

rabbit, rat, mouse, and shed snake skin, as well as artificial membranes such as Strat-M<sup>®</sup>, Epiderm<sup>™</sup>, EpiSkin<sup>™</sup>, and LabSkin<sup>™</sup>. In addition, cultured living human skin cells, such as keratinocytes and fibroblasts, have been employed to evaluate skin permeation (Todo, 2017; Neupane et al., 2020). Fish skin has emerged as an appealing option for permeation studies due to its ready availability at a reasonable price (four to twelve Euros per piece). In contrast, other animal membranes are less accessible in the market and tend to be more expensive. For example, sourcing pig skins requires specific farms, and ethics committee approval is necessary for investigating and

using animal skins such as mice, rats, and rabbits (Abd et al., 2016; Dusch et al., 2009; Özgüney et al., 2006; Kantarcı et al., 2005). The preparation of fish skin for permeation testing is also uncomplicated compared to animal or human skins.

Fish skin morphology comprises distinct layers, including the epidermis, dermis, hypodermis, and muscle. Notably, fish scales play a unique role as an important component of the dermal skeleton. The base of each fish scale is located within the dermis layer, while the head is covered by the epidermal tissue. The type, number, and size of scales serve as indicator of lifestyle traits. Fish species that swim rapidly in fast-flowing water often have a large number of scales (e.g., trout), whereas scaleless characteristics are observed in fish that prefer hiding in confined spaces like caves or crevices (e.g., many catfish and eels) (Drelich et al., 2018; Elliott, 2011). The epidermal mucus layer, the initial secretion from mucus-secreting cells, serves a defensive function against the surrounding environment. It acts as a protective barrier, guarding against pathogens and external threats (Dash et al., 2018).

The evaluation of the percutaneous permeation is a crucial consideration when selecting alternative skin models. Previous studies have used skin from various anatomical locations (e.g., ear, abdomen, arm, and leg) of different animals or artificial membranes for testing, with the choice of skin models aligned with the investigation's objective. In skin permeability studies, it is essential that the selected animal skins or synthetic membranes possess similar thickness and lipid components to human skin (Supe and Takudage, 2021). The stratum corneum (SC) of human skin consists of corneocytes (protein-rich dead cells) and intercellular lipids. Previous reports have identified three main classes of that lipid in the SC, namely ceramides, cholesterol, and free fatty acids while phospholipids are not presented in the SC. The protein components presented in the epidermal layer include profilaggrin, proline-rich proteins, involucrin, and loricrin (Bouwstra et al., 2021). Parameters such as permeation flux ( $J$ ), permeation coefficient ( $K_p$ ), and permeation lag-time ( $T_{lag}$ ) are commonly used to compare the permeability of different model skins (Wagner et al., 2001; Yokota and Kyotani, 2018). This study aimed to explore the feasibility of using different types of fish skin, including both scaled and scaleless fish, as alternative models for skin permeability experiments. Skin parameters such as thickness,  $J$ ,  $K_p$ , and  $T_{lag}$  of four different fish skins (trout (*Salmo trutta*), Norwegian salmon (*Salmo salar*), BIO salmon (*Salmo salar*), and bighead catfish (*Clarias macrocephalus*)) were compared.

## 2. MATERIALS AND METHODS

### 2.1 Materials

Fish skins (trout, Norwegian salmon, BIO salmon, and bighead catfish) were purchased from local supermarkets in Berlin, Germany. Shed snake skins (*Lampropeltis triangulum campbelli* (L.T.), *Epicrates maurus colombianus* (E.M.), and *Python regius* (P.R.)) were obtained from Reptilienpool, Germany. Pure caffeine powder (100%) was obtained from BASF (Monheim am Rhein, Germany). All chemical substances used were of analytical grade.

### 2.2 Preparation of caffeine standard solutions

A standard solution containing 1000 µg/mL of caffeine was prepared by dissolving caffeine in deionized water (DI) in a volumetric flask. The stock standard solution was then diluted with DI to prepare standard solutions at concentrations of 1, 5, 10, 20, 30, 40, and 50 µg/mL.

### 2.3 Determination of caffeine

The standard solutions at different concentrations were scanned from 200 to 400 nm wavelengths, and the absorbances were analyzed by a UV/vis spectrophotometer (Shimadzu UK Limited, UK). The wavelength with the highest spectrum, demonstrating linearity, was selected for detecting caffeine content.

The selected spectrum ( $\lambda$  max) was utilized to measure the caffeine content using UV/vis spectrophotometer (Camspec M508, Spectronic CamSpec Ltd, UK) based on the standard calibration curve.

### 2.4 Saturated solubility of caffeine

An excess of caffeine powder was added to a sealed glass bottle containing 10 mL of DI water and stirred using a magnetic stirrer. After reaching solid-liquid equilibrium, the mixture was filtered through a 0.45-µm syringe filter. The saturated solution was then diluted with DI, and the caffeine content was analyzed by a UV/vis spectrophotometer at 272 nm. The amount of caffeine was calculated from the standard calibration curve, as described above.

### 2.5 In vitro skin permeation study

The upper side, lateral line, and lower side of various fish skins (trout, Norwegian salmon, BIO salmon, and bighead catfish) were used as models for the skin permeation study. Each fish was sliced into two parts and the fishbone was removed. The hypodermis and muscle layers were then carefully cut out using a knife and a lancet. Only the epidermis and dermis skin layers were used as model membranes for the skin permeation study. The thickness of the trimmed fish skins was measured using a digital slide caliper with an accuracy of  $\pm 0.03$  mm (Tchibo, Hamburg, Germany). The catfish was scaleless, while the others fish types had scales that were not removed. The fish skins were separated into three areas: the upper side, lateral line, and lower side, and studied to determine differences in skin permeability. The skin permeation of caffeine was evaluated by vertical Franz-type diffusion cells. A 1% w/v solution of caffeine was dissolved in DI, and 5 mL of DI water as a receptor medium were continuously stirred using a magnetic stirrer at  $32 \pm 0.5$  °C. The skins were placed between the donor and receptor compartments. At different time intervals (0.5, 1, 2, 3, 4, 5, 6, and 7 h), 400 µL of the receptor medium was collected to quantify the caffeine content using a UV/vis spectrophotometer (Camspec M508, Spectronic CamSpec Ltd, UK) at 272 nm. The same volume of DI water was added to the receptor compartment to maintain a constant volume.

### 2.6 Determination of skin permeation parameters

Fick's law of diffusion was used as a mathematical model to calculate the skin permeation parameters, with  $J$  and  $K_p$  calculated by Equations 1 and 2, respectively (Kumpugdee-Vollrath et al., 2015).

$$J = \Delta m / (\Delta t \cdot A) \quad (1)$$

where  $\Delta m$  = the amount of substance being transported,  
 $\Delta t$  = time  
 $A$  = surface area

$$Kp = (D \cdot K) / d = J / C_D \quad (2)$$

where  $D$  = diffusion coefficient  
 $K$  = partition coefficient  
 $d$  = layer thickness  
 $C_D$  = caffeine concentration in the donor compartment

$T_{lag}$  is the lag time of diffusion. It is defined as the time taken before a penetrant's concentration at the skin barrier is transported through the dermal membrane and reaches steady-state permeation in the receptor compartment. The  $T_{lag}$  was obtained from the intersection of the graph of the cumulative amount per area and time profile ( $y = 0$ ) as:

$$T_{lag} = \text{Interception/slope} \quad (3)$$

## 2.7 Determination of fish skin composition

After preparation, the fish skins were dried at room temperature. The lipid and protein components of the skin samples were analyzed by an attenuated total reflectance-Fourier transform infrared spectrophotometer (ATR-FTIR, Nicolet iS5-iD7 (ATR), Thermo Scientific, USA) with a Perkin

Elmer Spectrum 100 FTIR spectrometer, serial number 77515 and universal ATR sampling accessory, serial number PODL07071830, using Perkin Elmer Spectrum, version 6.1.1.0045 software at room temperature.

## 2.8 Statistical analysis

All data were represented as the mean  $\pm$  standard deviation (S.D.), with significant statistical differences analyzed by one-way ANOVA followed by Tukey's post hoc test at  $p < 0.05$ .

## 3. RESULTS AND DISCUSSION

### 3.1 UV spectrum of caffeine

Caffeine content was determined by the spectrophotometric method. The UV spectrum of caffeine in deionized water was scanned at wavelengths ranging from 200 to 400 nm, with results presented in Figure 1. The spectrum of caffeine dissolved in deionized water presented three peaks at 219, 233, and 271 or 272 nm, with peaks at 271–272 nm correlating with Dobrinas et al. (2013). The peaks at 271 and 272 nm were also reported to evaluate the caffeine content in many other studies (Veryser et al., 2013; Amos-Tautua et al., 2014). The two spectra (271 and 272 nm) were confirmed for linearity, with the graph at wavelength number 272 nm more linear than at 271 nm. Therefore, the spectrum at 272 nm was used for further experiments.

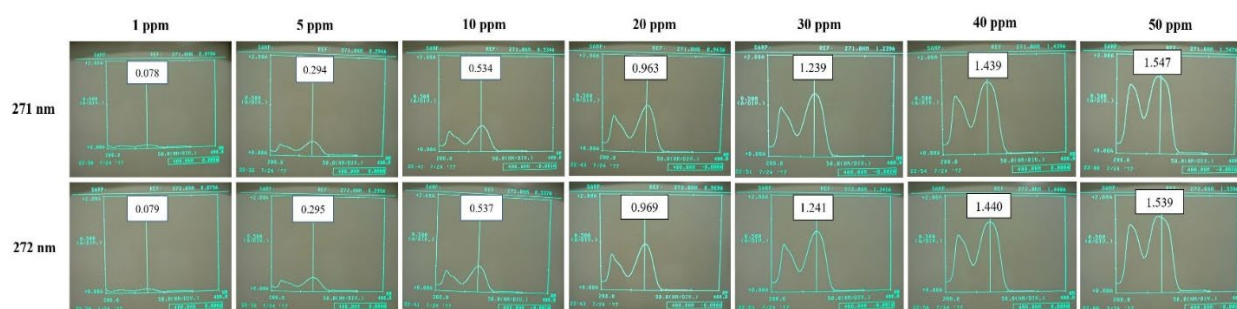


**Table 1.** UV spectra of caffeine solution scanned over the wavelength of 200–400 nm

### 3.2 Quantitative analysis of caffeine

Quantitative determination of caffeine was performed at 272 nm. The concentration of caffeine in DI water was varied from 1 to 50  $\mu\text{g/mL}$ . The concentration at 50  $\mu\text{g/mL}$  influenced the graphic trend but was non-linear (data not shown). The calibration curve of caffeine showed linearity over the range of 1 to 40  $\mu\text{g/mL}$ . The relationship between the concentration of standard caffeine solution and the UV absorbance was represented by the equation  $y = 0.0473x + 0.034$ , with the correlation factor ( $R^2$ ) of 0.9995.

### 3.3 Saturated solubility of caffeine

The saturated solubility of caffeine dissolved in water at 18.9  $^{\circ}\text{C}$  was  $20.52 \pm 0.57$  mg/mL, concurring with Vuong and Roach (2014), who reported that 2% w/v (21.7 mg/mL) was the saturated solubility of caffeine in water at 25  $^{\circ}\text{C}$ . The solubility at 25  $^{\circ}\text{C}$  was greater because caffeine solubility increased at higher temperatures (Zhong et al., 2017).

### 3.4 Permeation of caffeine in different fish skin areas and model types

The permeation characteristics of various fish skins have been studied over the past decade, comparing them with

artificial membranes, shed snake skins and mouse skins. Fish skin has a structure similar to human skin, consisting of the epidermis, dermis, hypodermis, and muscle layers (Elliott, 2011). However, some fish skin compositions differ, such as the presence of mucus and scales. Rakers et al. (2010) reported fish skin composition is similar to mammalian skin, such as mice or humans with the same layers, except mucus replaces keratinocytes. Pigmentation patterns (melanocytes), their progeny, and the generation of vertebrate skin appendages, such as hairs, feathers, and scales, also show similarities in some molecular pathways (Rakers et al., 2010). Catfish (*Anarichas lupus* L.) skin without tissue was used as a model membrane for permeation studies, with drug permeation through the mucosal membrane being diffusion-controlled, and mucus acting as the rate-limiting barrier (Konrádsdóttir et al., 2010). Lipophilic and hydrophilic molecules were used as model substances. Hydrophilic molecules tend to permeate fish skin more effectively than lipophilic molecules, utilizing hydrated channels or aqueous pores. Small lipophilic molecules ( $\text{MW} < 500$ ;  $\log P$  1–3), such as naproxen, lidocaine, and benzocaine, can permeate fish skin through aqueous pores or channels. Although, fish



skin is not a perfect substitute for human skin, it can be employed in permeation studies to offer valuable insights in certain contexts (Másson et al., 2002). The morphology and characteristics of the studied skin

samples are shown in Figure 2. The *in vitro* skin permeation of caffeine was assessed using three different areas of each fish skin: the upper side, lateral line, and lower side, as presented in Figure 3.

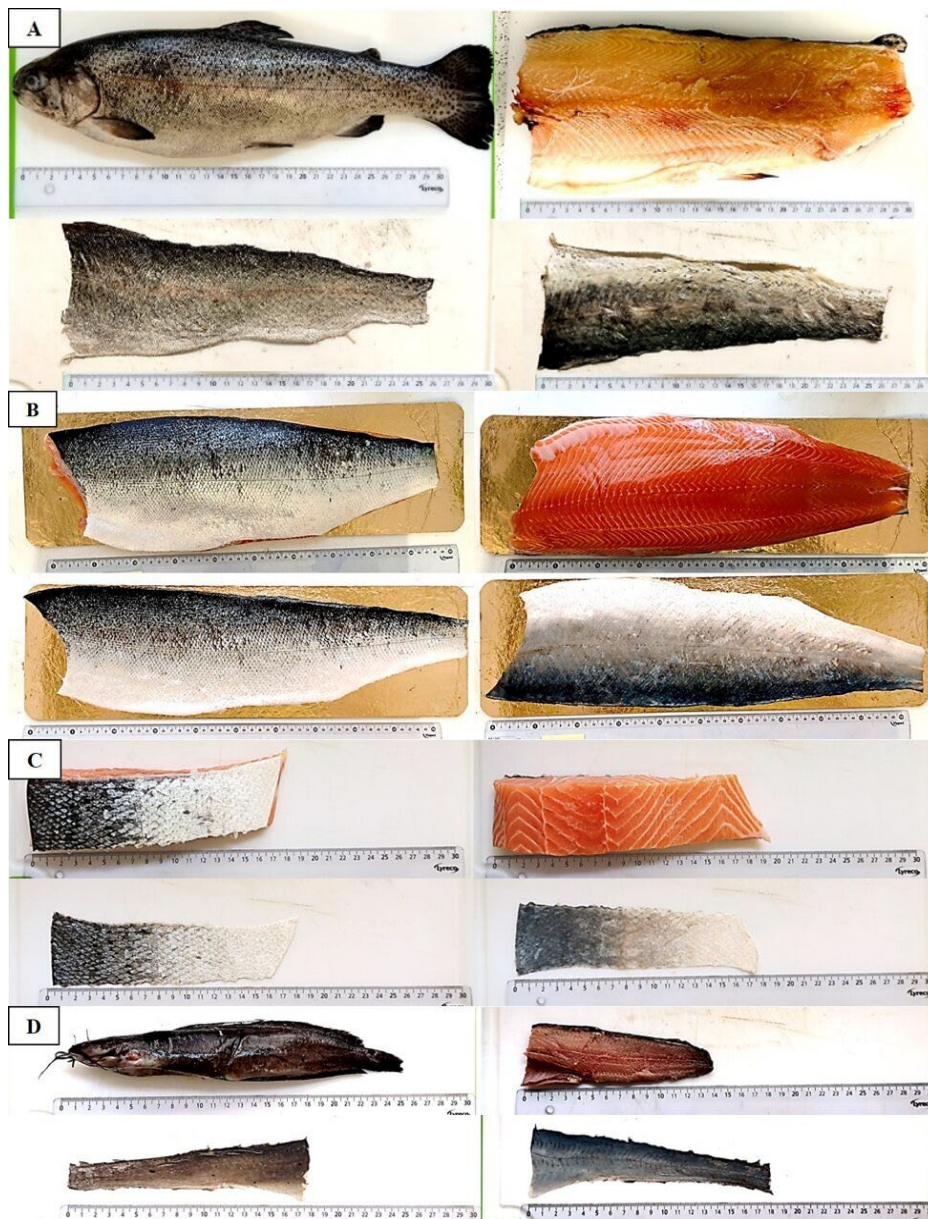


**Figure 2.** Morphology and characteristics of the model fish skins: (A) trout, (B) Norwegian salmon, (C) BIO salmon, and (D) bighead catfish

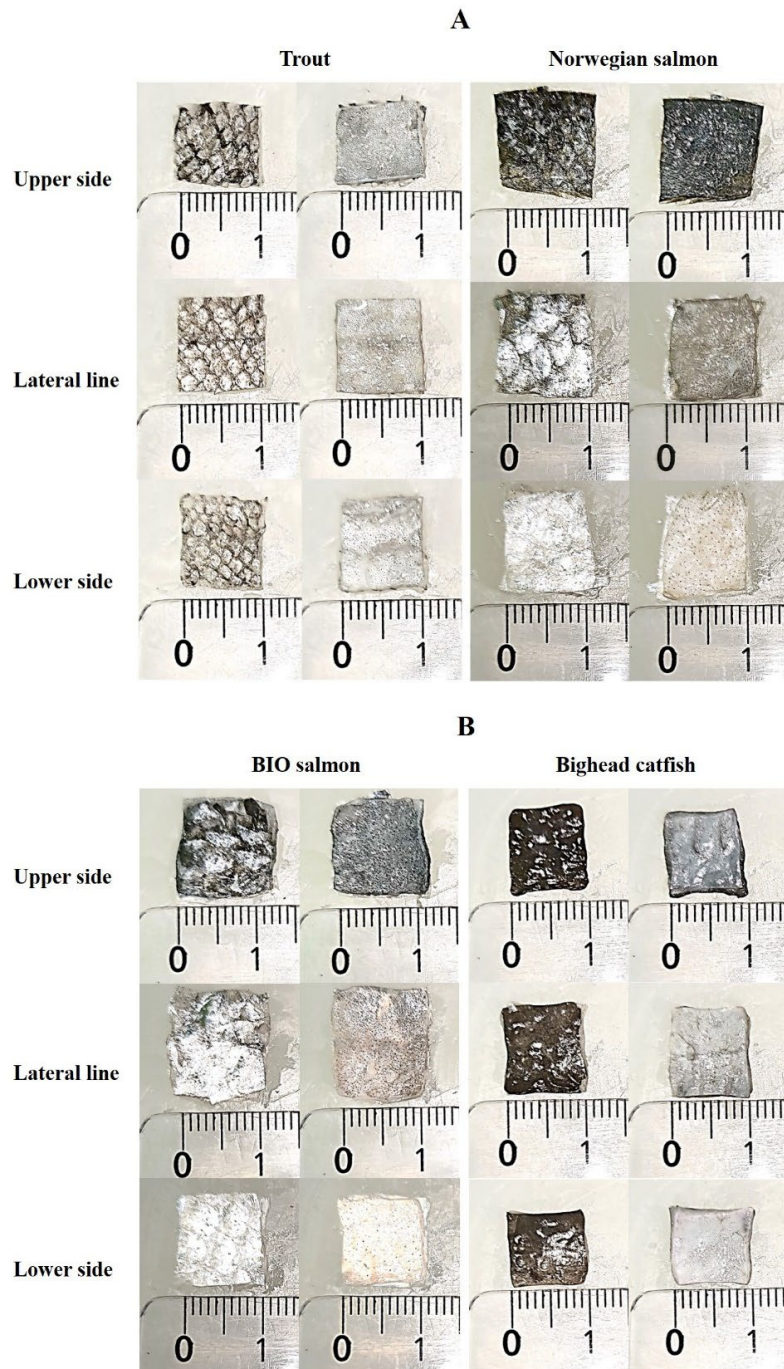


**Figure 3.** Photographs of three different parts (the upper side, the lateral line, and the lower side) of the different fish skin layers (trout, Norwegian salmon, BIO salmon and bighead catfish)

The cumulative permeation profile of caffeine over time, obtained from the skin permeation study, is displayed in Figure 4. The results indicate that all areas of bighead catfish skins delivered more caffeine through the skin compared to the other fish skins. The upper side of the bighead catfish showed the highest drug permeated amounts compared to the other fish types ( $p < 0.05$ ). The bighead catfish membrane demonstrated higher permeation of caffeine than the other fish membranes, attributed to its thin skin and lack of scales. Másson et al. (2002) conducted a skin permeation experiment using

catfish skin for various drugs, and found that catfish membrane exhibited high permeability for small molecules, which permeated through aqueous channels. Electron microscopy cross-section images of catfish skin showed large intercellular spaces, allowing rapid and high permeation of small molecules through the aqueous pores in the catfish membrane (Másson et al., 2002). Caffeine, composed of small molecules with high water solubility, demonstrated effective permeation through bighead fish skin. However, it should be noted that different biological chromophores in human skin exhibit diverse absorption



spectra. Proteins, in particular, exhibit a characteristic UV absorption maximum spectrum at 280 nm, particularly in aromatic amino acids, such as tyrosine and tryptophan (Proykova et al., 2018). Fish scales, being composed of gelatin, can yield peptide bond fragments detected by a UV/vis spectrophotometer, with chromophore groups

exhibiting absorption in the range of 210–240 nm. Das et al. (2017) reported a peak spectrum at 224 nm. The measurement of caffeine content at 273 nm might be influenced by skin chromophores, such as tyrosine and tryptophan, and the cumulative permeation of caffeine may reflect the sum of caffeine and proteins.

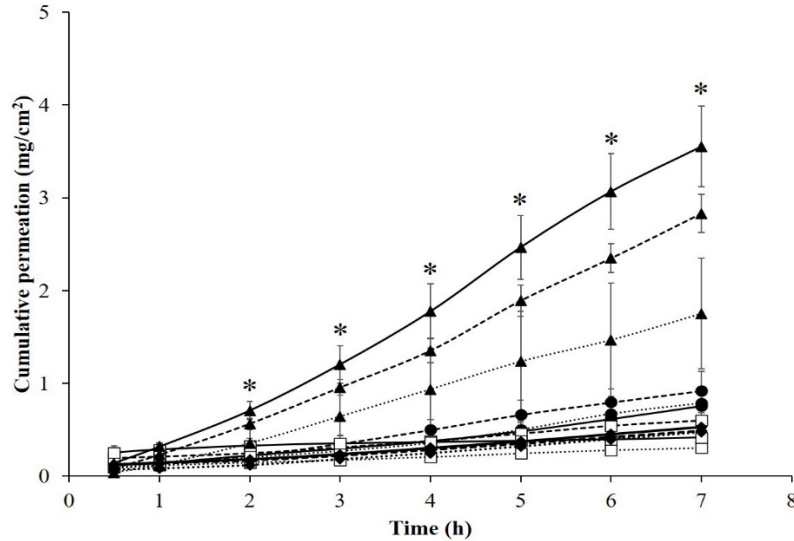


**Figure 4.** Cumulative permeation profile of 1% w/v caffeine solution permeated through the skin of trout (●), Norwegian salmon (□), bighead catfish (▲), and BIO salmon (◆) in three different parts: upper side (—), lateral line (.....), and lower side (— — —)

Note: Data are plotted as the mean±SD of six measurements. \* Statistically significant ( $p < 0.05$ )

Permeability parameters were calculated from the skin permeation profiles, with  $J$ ,  $K_p$ , and  $T_{lag}$  values being dependent on the fish type and skin areas. The calculated permeation parameters are listed in Table 1. The thickness of the skin membranes varied from 173 to 498  $\mu\text{m}$ . The thickness of the skin membrane had an impact on drug permeability through the skin. When comparing the flux and permeability coefficients among different skin membranes, bighead catfish membranes displayed higher values than others due to their thinner skins. Thickness is an important factor that affects the permeability of fish skin. Drugs permeate more easily through thin skin compared to thick skin. However, additional factors, such as fish type and skin area, also influence permeability.

The commercial synthetic membrane (Strat-M®) has also been used in skin permeation experiments involving caffeine solution with water as the receptor medium. Permeability parameters for caffeine solution using Strat-M® are summarized in Table 2. To facilitate a comparison of the permeability across Strat-M® and various types of fish skin, the data were normalized into a ratio relative to Strat-M®. Table 3 shows skin thickness sorted based on proximity to Strat-M®. Fish skins providing values closest to Strat-M® in descending order were lower Norwegian salmon > upper Norwegian salmon  $\approx$  lateral Norwegian salmon  $\approx$  upper trout  $\approx$  lower trout > lower BIO salmon > upper bighead catfish > lateral trout > lateral bighead catfish  $\approx$  lower bighead catfish > upper BIO salmon > lateral BIO salmon. The  $J$  and  $K_p$  values giving the closest values to Strat-M® were lateral Norwegian salmon > upper Norwegian salmon > lower BIO salmon > lateral BIO salmon > upper BIO salmon > lower Norwegian salmon >

upper trout > lateral trout > lower trout > lateral bighead catfish > lower bighead catfish > upper bighead catfish. Unfortunately,  $T_{lag}$  values could not be compared as the reference article did not report the  $T_{lag}$  value of Strat-M®. Notably, the lateral side of Norwegian salmon exhibited values similar to Strat-M®.

### 3.5 Composition of fish skin membrane

The stratum corneum (SC) and viable epidermis were characterized to provide information on skin permeation. The main structural components of the SC form the brick-and-mortar system, where corneocytes act as bricks and intercellular lipids as mortar (Menon et al., 2012). As the outermost layer of the epidermis, the SC serves as the main barrier to epidermal permeability. Free fatty acids (FFAs) are not only absorbed by the epidermis but also contribute to the synthesis of ceramides and acyl-ceramide. FFAs can transform into acyl-glucosylceramides, sphingomyelin, and phospholipids. Moreover, the epidermis also plays an important role in cholesterol synthesis, phospholipids are generated from ceramides and cholesterol within the epidermal keratinocytes (Bhattacharya et al., 2019). Free ceramides found in the human SC include CER EOS/DS, CER NS/DS, CER EOP, CER NP, CER EOH, CER AS/DS, CER NH, CER AP, and CER AH (Ponec et al., 2003). Corneocytes are composed of tightly bundled keratin filaments arranged parallel to the skin surface and encased by a cornified envelope (CE). Each keratin intermediate filament binds together with filaggrin, and some filaggrin crosslink with CE proteins. During the formation of a CE in epidermal cells, the precursor proteins consist mostly of loricrin and interconnecting small proline-rich proteins

(SPRs). Involucrin is also widely presented in stratified squamous epithelium and is associated with the creation of CEs (Nemes and Steinert, 1999). As presented in Figure 5, all fish skins exhibited peaks at 3200–3300, 1620–1650, 1510–1550, and 1450  $\text{cm}^{-1}$ . Human skin and fish skin showed high intensities of peaks at 2920, 2850, and 1740  $\text{cm}^{-1}$  (Sviridov et al., 2004), indicating lipid chain conformations. However, shed snake skins showed low intensity peaks at 2920 and 2850  $\text{cm}^{-1}$ , and the peak at 1740  $\text{cm}^{-1}$  was absent. The peak at 3200–3300  $\text{cm}^{-1}$  was attributed to O-H stretching of water molecules (3200  $\text{cm}^{-1}$ ) or N-H stretching of keratinized proteins (3300  $\text{cm}^{-1}$ ) (Barry et al., 1992; Laugel et al., 2005). Stretching vibrations at 2920 and 2850  $\text{cm}^{-1}$  were due to asymmetric  $\text{CH}_2$  stretching and symmetric  $\text{CH}_2$  stretching, commonly detected in lipid chain conformation of human SC such as ceramides (Moore and Rerek, 2000; Pensack et al., 2006).

The peak at 1740  $\text{cm}^{-1}$  indicated the presence of unsaturated lipid skin structure (triglycerides or phospholipids) because this spectrum is related to the ester structure (Mendelsohn et al., 2006). The absence of the peak at 1740  $\text{cm}^{-1}$  in shed snake skins signifies that these skins lack of unsaturated lipid structure. Ceramide amide I and II were found at 1650 and 1550  $\text{cm}^{-1}$ , respectively (Moore and Rerek, 2000). The peaks at 1450  $\text{cm}^{-1}$  were due to the  $\text{CH}_2$  scissoring modes of ceramide or asymmetric  $\text{CH}_3$  scissoring (Barry et al., 1992; Gorcea et al., 2012), while the band at 1080  $\text{cm}^{-1}$  corresponded to the  $\text{CD}_2$  scissoring mode of fatty acids. Peaks at wavenumbers less than 1300  $\text{cm}^{-1}$  were very weak and not clearly presented in the IR spectrum (Barry et al., 1992; Gorcea et al., 2012). Based on the IR spectrum, fish skins were shown to be closer to human skin (Sviridov et al., 2004) than shed snake skins.

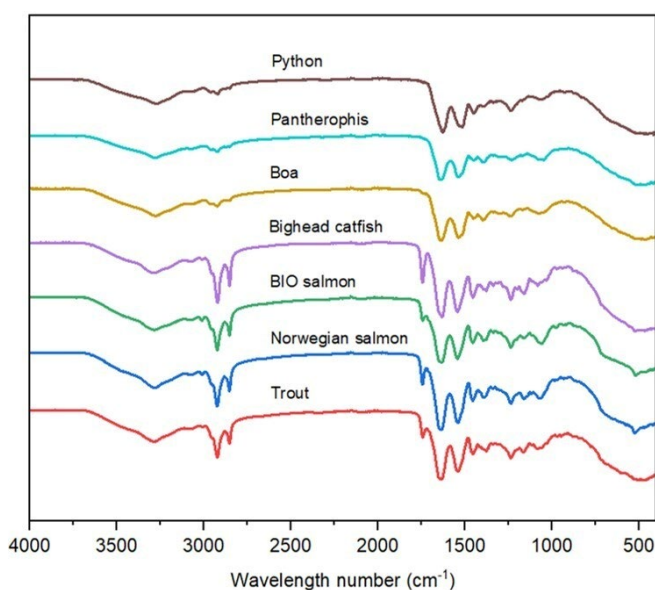


**Figure 5.** FT-IR spectra of animal skins: fish skins (trout, Norwegian salmon, BIO salmon, and bighead catfish) and shed snake skins (Boa, Pantherophis, and Python)

#### 4. CONCLUSION

The study investigated the permeability parameters of four fish skin membranes. The ATR-FTIR spectra indicated that fish skins were more similar to human skin than shed snake skins. The data analysis of ATR-FTIR provided information on the main components of skin, demonstrating similarities to human skin. The permeation abilities of fish skins were found to be comparable to Strat-M® under the same conditions. The results suggest that the lateral side of Norwegian salmon skin could serve as alternative membrane for studying skin permeability in place of Strat-M®.

#### ACKNOWLEDGMENT

We acknowledge the use of research instruments supplied by the Department of Pharmaceutical and Chemical Engineering, Berliner Hochschule für Technik, Berlin, Germany and the Department of Industrial Pharmacy, Faculty of Pharmacy, Silpakorn University, Nakhon Pathom,

Thailand. We are also grateful for financial support from the Thailand Research Fund through the National Research Council of Thailand (NRCT): N42A650551.

#### REFERENCES

- Abd, E., Yousef, S. A., Pastore, M. N., Telaprolu, K., Mohammed, Y. H., Namjoshi, S., Grice, J. E., and Roberts, M. S. (2016). Skin models for the testing of transdermal drugs. *Clinical Pharmacology: Advances and Applications*, 8, 163–176.
- Amos-Tautua, B., Martin, W., and Ere, D. (2014). Ultra-violet spectrophotometric determination of caffeine in soft and energy drinks available in Yenagoa, Nigeria. *Advance Journal of Food Science and Technology*, 6(2), 155–158.
- Arce, F. J., Asano, N., See, G. L., Itakura, S., Todo, H., and Sugibayashi, K. (2020). Usefulness of artificial membrane, Strat-M®, in the assessment of drug permeation from complex vehicles in finite dose conditions. *Pharmaceutics*, 12(2), 173.



- Barry, B. W., Edwards, H. G. M., and Williams, A. C. (1992). Fourier transform Raman and infrared vibrational study of human skin: Assignment of spectral bands. *Journal of Raman Spectroscopy*, 23(11), 641–645.
- Bhattacharya, N., Sato, W. J., Kelly, A., Ganguli-Indra, G., and Indra, A. K. (2019). Epidermal lipids: key mediators of atopic dermatitis pathogenesis. *Trends in Molecular Medicine*, 25(6), 551–562.
- Bouwstra, J. A., Helder, R. W. J., and El Ghalbzouri, A. (2021). Human skin equivalents: Impaired barrier function in relation to the lipid and protein properties of the stratum corneum. *Advanced Drug Delivery Reviews*, 175, 113802.
- Das, M. P., R., S. P., Prasad, K., J. V., V., and M, R. (2017). Extraction and characterization of gelatin: a functional biopolymer. *International Journal of Pharmacy and Pharmaceutical Sciences*, 9(9), 239–242.
- Dash, S., Das, S. K., Samal, J., and Thatoi, H. N. (2018). Epidermal mucus, a major determinant in fish health: A review. *Iranian Journal of Veterinary Research*, 19(2), 72–81.
- Dobrinás, S., Soceanu, A., Popescu, V., Stanciu, G., and Smalberger, S. A. (2013). Optimization of a UV-VIS spectrometric method for caffeine analysis in tea, coffee and other beverages. *Scientific Study & Research: Chemistry & Chemical Engineering, Biotechnology, Food Industry*, 14(2), 071–078.
- Drelich, A. J., Monteiro, S. N., Brookins, J., and Drelich, J. W. (2018). Fish skin: A natural inspiration for innovation. *Advanced Biosystems*, 2(7), 1800055.
- Dusch, M., Schley, M., Obreja, O., Forsch, E., Schmelz, M., and Rukwied, R. (2009). Comparison of electrically induced flare response patterns in human and pig skin. *Inflammation Research*, 58(10), 639–648.
- Elliott, D. G. (2011). The skin: Functional morphology of the integumentary system in fishes. In *Encyclopedia of Fish Physiology* (P. F. Anthony, Ed.), (pp. 476–488). Cambridge, MA: Academic Press.
- Gorcea, M., Hadgraft, J., Moore, D. J., and Lane, M. E. (2012). Fourier transform infrared spectroscopy studies of lipid domain formation in normal and ceramide deficient stratum corneum lipid models. *International Journal of Pharmaceutics*, 435(1), 63–68.
- Kantarci, G., Özgüney, I., Karasulu, H. Y., Güneri, T., and Başdemir, G. (2005). In vitro permeation of diclofenac sodium from novel microemulsion formulations through rabbit skin. *Drug Development Research*, 65(1), 17–25.
- Konrádsdóttir, F., Loftsson, T., and Sigfússon, S. D. (2010). Fish skin as a model membrane: Structure and characteristics. *Journal of Pharmacy and Pharmacology*, 61(1), 121–124.
- Kumpugdee-Vollrath, M., Phu, T. G. D., and Helms, M. (2015). Effect of different model drugs on the properties of model membranes from fishes. *World Academy of Science, Engineering, and Technology International Journal of Animal and Veterinary Sciences*, 9(7), 855–859.
- Laugel, C., Yagoubi, N., and Baillet, A. (2005). ATR-FTIR spectroscopy: A chemometric approach for studying the lipid organisation of the stratum corneum. *Chemistry and Physics of Lipids*, 135(1), 55–68.
- Másson, M., Sigfússon, S. D., and Loftsson, T. (2002). Fish skin as a model membrane to study transmembrane drug delivery with cyclodextrins. *Journal of Inclusion Phenomena and Macrocyclic Chemistry*, 44(1), 177–182.
- Mendelsohn, R., Flach, C. R., and Moore, D. J. (2006). Determination of molecular conformation and permeation in skin via IR spectroscopy, microscopy, and imaging. *Biochimica et Biophysica Acta (BBA) - Biomembranes*, 1758(7), 923–933.
- Menon, G. K., Cleary, G. W., and Lane, M. E. (2012). The structure and function of the stratum corneum. *International Journal of Pharmaceutics*, 435(1), 3–9.
- Moore, D. J., and Rerek, M. E. (2000). Insights into the molecular organization of lipids in the skin barrier from infrared spectroscopy studies of stratum corneum lipid models. *Acta Dermato-Venereologica*, 80(208 Suppl.), 16–22.
- Özgüney, I. S., Karasulu, H. Y., Kantarci, G., Sözer, S., Güneri, T., and Ertan, G. (2006). Transdermal delivery of diclofenac sodium through rat skin from various formulations. *Journal of the American Association of Pharmaceutical Scientists*, 7(4), E39–E45.
- Nemes, Z., and Steinert, P. M. (1999). Bricks and mortar of the epidermal barrier. *Experimental & Molecular Medicine*, 31(1), 5–19.
- Neupane, R., Boddu, S. H. S., Renukuntla, J., Babu, R. J., and Tiwari, A. K. (2020). Alternatives to biological skin in permeation studies: Current trends and possibilities. *Pharmaceutics*, 12(2), 152.
- Pensack, R. D., Michniak, B. B., Moore, D. J., and Mendelsohn, R. (2006). Infrared kinetic/structural studies of barrier reformation in intact stratum corneum following thermal perturbation. *Applied Spectroscopy*, 60(12), 1399–1404.
- Ponec, M., Weerheim, A., Lankhorst, P., and Wertz, P. (2003). New acylceramide in native and reconstructed epidermis. *Journal of Investigative Dermatology*, 120(4), 581–588.
- Proykova, A., Samaras, T., Ion, R.-M., Bruzell, E. M., Doré, J.-F., Nicolo, M., O'Hagan, J., Sánchez-Ramos, C., and van Kerkhof, L. (2018). *Potential Risks to Human Health of LEDs (Final Opinion)*, Luxembourg: European Commission, pp. 1–92.
- Rakers, S., Gebert, M., Uppalapati, S., Meyer, W., Maderson, P., Sell, A. F., Kruse, C., and Paus, R. (2010). 'Fish matters': The relevance of fish skin biology to investigative dermatology. *Experimental Dermatology*, 19(4), 313–324.
- Ramadon, D., McCrudden, M. T. C., Courtenay, A. J., and Donnelly, R. F. (2022). Enhancement strategies for transdermal drug delivery systems: current trends and applications. *Drug Delivery and Translational Research*, 12(4), 758–791.
- Sviridov, A. P., Zimnyakov, D. A., Sinichkin, Y. P., Butvina, L. N., Omelchenko, A. J., Shakh, G. S., and Bagratashvili, V. N. (2004). Attenuated total reflection Fourier transform infrared and polarization spectroscopy of in vivo human skin ablated, layer by layer, by erbium:YAG laser. *Journal of Biomedical Optics*, 9(4), 820–827.
- Supe, S., and Takudage, P. (2021). Methods for evaluating penetration of drug into the skin: A review. *Skin Research and Technology*, 27(3), 299–308.
- Todo, H. (2017). Transdermal permeation of drugs in various animal species. *Pharmaceutics*, 9(3), 33.
- Veryser, L., Boonen, J., Mehuys, E., Roche, N., Remon, J.-P., Peremans, K., Burvenich, C., and De Spiegeleer, B. (2013). Transdermal evaluation of caffeine in different



- formulations and excipients. *Journal of Caffeine Research*, 3(1), 41–46.
- Vuong, Q., and Roach, P. D. (2014). Caffeine in green tea: Its removal and isolation. *Separation and Purification Reviews*, 43(2), 155–174.
- Wagner, H., Kostka, K.-H., Lehr, C.-M., and Schaefer, U. F. (2001). Interrelation of permeation and penetration parameters obtained from in vitro experiments with human skin and skin equivalents. *Journal of Controlled Release*, 75(3), 283–295.
- Yokota, J., and Kyotani, S. (2018). Influence of nanoparticle size on the skin penetration, skin retention and anti-inflammatory activity of non-steroidal anti-inflammatory drugs. *Journal of the Chinese Medical Association*, 81(6), 511–519.
- Zhong, J., Tang, N., Asadzadeh, B., and Yan, W. (2017). Measurement and correlation of solubility of theobromine, theophylline, and caffeine in water and organic solvents at various temperatures. *Journal of Chemical & Engineering Data*, 62(9), 2570–2577.

**Table 1.** Permeability data (means $\pm$ S.D.) of 1% w/v caffeine solution across the different parts of the trout, Norwegian salmon, bighead catfish, and BIO salmon skin layers (n = 6)

Parameter	Trout			Norwegian salmon			BIO salmon			Bighead catfish		
	Upper	Lateral	Lower	Upper	Lateral	Lower	Upper	Lateral	Lower	Upper	Lateral	Lower
Thickness ( $\mu\text{m}$ )	427 $\pm$ 18.62	438 $\pm$ 42.62	417 $\pm$ 30.77	428 $\pm$ 26.39	428 $\pm$ 7.53	372 $\pm$ 17.22	478 $\pm$ 23.17	498 $\pm$ 54.56	437 $\pm$ 45.02	173 $\pm$ 20.66	192 $\pm$ 14.72	188 $\pm$ 16.02
$J$ ( $\times 10^3$ ) ( $\mu\text{g}\cdot\text{cm}^{-2}\cdot\text{h}^{-1}$ )	0.10 $\pm$ 0.02	0.11 $\pm$ 0.02	0.13 $\pm$ 0.03	0.05 $\pm$ 0.01	0.03 $\pm$ 0.00	0.06 $\pm$ 0.02	0.06 $\pm$ 0.01	0.06 $\pm$ 0.01	0.06 $\pm$ 0.01	0.54 $\pm$ 0.07	0.27 $\pm$ 0.03	0.43 $\pm$ 0.10
$K_p$ ( $\text{cm}\cdot\text{h}^{-1}$ )	0.22 $\pm$ 0.04	0.26 $\pm$ 0.07	0.31 $\pm$ 0.09	0.10 $\pm$ 0.02	0.08 $\pm$ 0.01	0.17 $\pm$ 0.06	0.13 $\pm$ 0.02	0.13 $\pm$ 0.03	0.13 $\pm$ 0.04	3.19 $\pm$ 0.75	1.30 $\pm$ 0.16	2.25 $\pm$ 0.57
$T_{\text{lag}}$ (min)	Immediate release			Immediate release			Immediate release			30.60 $\pm$ 4.02	31.80 $\pm$ 7.33	33.70 $\pm$ 8.60

**Table 2.** *In vitro* skin permeability parameters (thickness,  $J$ ,  $K_p$ , and  $T_{\text{lag}}$ ) and *in vitro* skin permeation test conditions (caffeine concentration, vehicle, medium, and temperature) of Strat-M® (Arce et al., 2020)

Thickness ( $\mu\text{m}$ )	$J$ ( $\mu\text{g}\cdot\text{cm}^{-2}\cdot\text{h}$ )	$K_p$ ( $\times 10^{-4}$ ) ( $\text{cm}\cdot\text{h}$ )	$T_{\text{lag}}$ (min)	Caffeine	Vehicle	Medium	Temperature
324.6	20.94 - 24.01	26.10 - 29.88	data not available	0.7 - 1%	Water	Water	32 °C

**Table 3.** Skin permeability parameters (thickness,  $J$ ,  $K_p$ , and  $T_{\text{lag}}$ ) of various type of fish skins based on the relative value to Strat-M®

Parameter	Strat-M®	Fish types											
		Trout			Norwegian salmon			BIO salmon			Bighead catfish		
		Upper	Lateral	Lower	Upper	Lateral	Lower	Upper	Lateral	Lower	Upper	Lateral	Lower
Thickness	1	1.32	1.39	1.32	1.32	1.32	1.14	1.48	1.54	1.36	0.62	0.58	0.58
<i>J</i>	1	3.96	4.67	5.32	1.95	1.34	2.68	2.62	2.60	2.38	22.56	11.24	17.73
<i>K</i> p (x10 <sup>3</sup> )	1	13.10	15.48	17.63	6.46	4.45	8.88	8.69	8.62	7.90	74.73	37.21	58.72

\*The values of  $T_{\text{lag}}$  are unable to be calculated because the value of Strat-M® was not reported in the reference article